Rheological and Rheo-Optical Characterization of Asphalt Cement and Evaluation of Relaxation Properties

DALLAS N. LITTLE, ALAN LETTON, S. PRAPNNACHARI, AND Y. RICHARD KIM

The rheological properties of asphalt depend on its molecular structure and chemical composition. The widely used Corbett fractions provide the composition of asphalt but lack the detailed structure/property relationships needed to accurately design asphalt systems. Depending on the proportions of the generic fractions, an asphalt is either a dispersed type or a solution type. The dispersed type is also termed micellar or colloidal; the solution type is termed "polymer type." The literature is unclear as to which structure accurately represents the mechanical behavior of an asphalt system. Material science tools are used to elucidate the structure of asphalt. In particular, a rheo-optical technique was developed and used to probe changes in molecular vibrations via Fourier transform infrared spectroscopy (FTIR) during shear deformation. The objective is to identify the important chemical aspects of an asphalt molecule that are related to the deformation properties of the asphalt. To clarify this relationship, detailed viscoelastic characterization of the asphalt was conducted to ensure an understanding of the asphalt's rheological properties. The FTIR results suggest an important link between rheological performance and linear structures in the asphalt cement complex. This concept was further probed through small-angle X ray scattering. Fractal analysis was used to determine the Porod scattering dimension, which is a measure of the dimensionality of the tested structure (i.e., whether it is linear or branched, or three-dimensionally branched).

Asphaltenes are proposed to be colloids (or micelles) dispersed in an oily medium peptized by resins. The peptizing ability of resins keeps asphaltenes, the highly associated component of asphalt, dispersed in the oily phase. The asphaltene fraction is the solute, and the other fractions combined (called maltenes) make up the solvent. There is limited consensus among researchers as to whether the asphaltene or the maltene contributes more to the overall physical behavior of an asphalt. Corbett described asphaltenes as solution thickeners that raise the asphalt's viscosity, and the other fractions have been described as being responsible for the ductility and fluidity of asphalt (*1*). Dealy (*2*) found asphaltenes to be the structuring component of asphalt and to play a key role in the rheological behavior of asphalt. Conversely, Boduszynski et. al. (*3*) found that asphaltenes lacked an independent rheological identity. They indicated that, because of the presence of the solvents, asphaltenes conglomerate as a highly associated phase; their study also indicated similarity in the molecular weights of asphaltenes and saturates (*3*). Petersen (*4*), referring to the work of Boduszynski et. al. (*3*), emphasized the role of compatibility among the four generic fractions of an asphalt. Halstead (*5*) reviewed the work of Boduszynski et al. and Petersen and found that it is the intercomponent relationship among the generic fractions that controls the overall physical properties of an asphalt, not simply the quantity of any single component. The functionality and the molecular structure are two main factors that determine the balance among the components of an asphalt (*4*). The microstructural model developed by Strategic Highway Research Program (SHRP) researchers is based on the hypothesis of a dispersed polar fluid (DPF) (*6*).

To predict the long-term performance properties of the asphalt, the microstructure of the whole asphalt, containing all the fractions together, must be known. Monismith (*7*) proposed two physical models to explain the chemical composition of asphalt. The first is the colloid or the micellar model, presented earlier, where the asphaltenes are held as discrete lumps by the peptizing ability of the resins (polar aromatics and naphthene aromatics) in the oil (saturates) medium. In the solution model, it is proposed that asphaltenes are dissolved in the oil-resin phase. The colloidal model has been more popular than the solution model as asphalt has been shown to deviate from true solution behavior (*5*).

Recently, SHRP announced its findings on the microstructure of asphalt studied using nuclear magnetic resonsance (NMR) and chromatography techniques. The DPF model pictures asphalt as a continuous, three-dimensional association of polar molecules dispersed in a fluid of nonpolar or relatively low-polarity molecules. Sulfur, nitrogen, and oxygen are incorporated in asphalt molecular substituents in the form of polar functional groups that are attached to hydrocarbon molecules. Many of the polar functional groups will behave as either acids or bases, and all are capable of forming dipolar, intermolecular bonds of varying strength with functional groups of opposite polarity. In this model, the viscoelastic properties of the asphalt and the response of asphalt to load- and temperature-induced stresses result directly from the making and breaking of bonds between polar molecules or other properties associated with a molecular superstructure. When the asphalt is subjected to stress, these secondary bonds are broken and reformed continuously. (This suggests the existence of a yield stress that could be probed using a stress-controlled rheometer.)

The DPF model proposed by SHRP differs from the older micellar model in several important ways. First, the micellar model postulates that asphalt is a collodial system with particles that are very large on a molecular scale—representing an agglomeration of many individual asphalt substituents (*6*). By contrast, the DPF model postulates no large assemblages. Rather, microstructural interactions depend on the wide variety of polar molecules dispersed

D. N. Little, A. Letton, and S. Prapnnachari, Texas Transportation Institute, Texas A&M University, TTI/CE Building, College Station, Tex. 77843-3135. Y. R. Kim, North Carolina State University, Box 7908, Mann Hall, Raleigh, N.C. 27695.

in the asphalt (*6*). NMR analysis has failed to find any large-scale assemblages.

Second, in the micellar model, colloidal particles are considered to be relatively permanent assemblages suspended in a dispersing medium. Because the electron density should vary between the colloidal and the suspending fluid, X ray scattering should demonstrate the presence of a colloidal system (*6*). The DPF model, conversely, proposes a structure that is continually forming and reforming as energy flows to and from the asphalt through media of external loading and temperature fluctuations (*6*).

Finally, the DPF model stresses the importance of polar asphalt molecules in mediating performance to a larger degree than the micellar model. A major component of the DPF model—producing a major influence over the formation of the molecular matrix—is the amphoteric. These molecules act as both an acid and a base and can thus associate extensively because they can fasten to other molecules at two or more sites instead of one (*6*).

The proposition of a network of molecules floating in a nonpolar fluid was investigated in this study.

VISCOELASTIC CHARACTERIZATION

Overview

Usually, strain-controlled, static tests are used to study the viscoelastic relaxation of a material. This type of test is particularly suitable for materials that are more elastic than viscous. For materials showing considerable viscous behavior, use of a strain-controlled, static test may be limited by extremely short experiment times. Asphalt exhibits both viscous and elastic properties depending on temperature and deformation rate. Dynamic mechanical tests overcome these constraints and, therefore, were used to characterize the asphalts studied here. Interconversions between viscoelastic functions are well documented in the literature and were used in this study to predict time-dependent properties.

To facilitate interconversion between time- and frequency-dependent linear viscoelastic functions, master curves of the storage (G') and loss (G'') moduli were constructed and used to calculate the discrete relaxation spectrum for each asphalt. The discrete function is related to the master curve through the following expressions:

$$G(t) = \sum_{i=1}^{z} G_i \, e^{\frac{-\tau}{\tau_i}}$$

$$G'(\omega) = \sum_{i=1}^{z} \frac{G_i \omega^2 \tau_i^2}{1 + \omega^2 \tau_i^2}$$

$$G''(\omega) = \sum_{i=1}^{z} \frac{G_i \omega \tau_i}{1 + \omega^2 \tau_i^2}$$

The G_i's and corresponding τ_i's make up the discrete relaxation spectra. A nonlinear algorithm is used to calculate a unique set of G_i's and τ_i's. The number of discrete nodes (τ_i values) is selected to provide a good fit to G' and G''. If the G_i's and τ_i's are known from the G' and G'' master curves, $G(t)$, the relaxation modulus, can be calculated straightforwardly. Similarly, the compliance function can be determined using the approximation

$$J_1 = \frac{1}{G_c} \text{ then } J(\tau) = \sum_{i=1}^{z} J_i(1 - e^{-\tau/\tau_i})$$

The relaxed modulus, G_R [$G(t = \infty)$], and the zero shear viscosity, η_0, are synonymous in characterizing the long-term behavior of a material (η_0 is proportional to the longest relaxation time). The relaxed modulus or equilibrium modulus is the stiffness of a material under a sustained deformation at an infinitely long time. The relaxed modulus is indeed the long-term resistance of a material against flow. For the range of frequencies and temperatures used in this study, the asphalt's equilibrium modulus was not obtainable. For this reason, the study of zero shear viscosity was an essential alternative to evaluate the long-term resistance against flow. The zero shear viscosity is approximated as follows:

$$\eta_0 = \sum_{i=1}^{z} G_i \tau_i$$

Prapnnachari (*8*) provides more detailed information about the viscoelastic characterization performed in this study.

Since the procedure for dynamic measurements on the Rheometrics Mechanical Spectrometer (RMS) is well established (*9,10*), it will not be repeated here. The asphalts tested were characterized over temperatures ranging from −25°C to 65°C and at frequencies ranging from 0.1 to 100 rad/sec. Details of the testing procedure are discussed by Little et al. (*11*).

Master curves and discrete relaxation spectra were constructed for each asphalt (*12*). The discrete relaxation spectra were used to calculate steady state or zero shear viscosity. Table 1 summarizes the zero shear viscosity for the asphalts tested.

Asphalts Analyzed

Eleven asphalts representing different sources were tested (*8*) using an RMS. For purposes of simplification in identification of data, asphalts studied are referred to as Type A, B, C, D, E, F, G, H, I, J, and K in lieu of identification by the asphalt's commercial name. The identification key for these asphalts is as follows:

Type	*Identification*
A	SHRP Asphalt AAA (AC-20)
B	SHRP Asphalt AAG (AC-20)
C	SHRP Asphalt AAM (AC-20)
D	Conoco AC-20
E	Frontier AC-20
F	Conoco AC-10
G	Frontier AC-10
H	Sinclair AC-10
I	Exxon AC-20
J	Santa Maria AC-10
K	Coastal AR-4000

MICROSTRUCTURAL MECHANICS BY RHEO-OPTICAL/FOURIER TRANSFORM INFRARED SPECTROSCOPY STUDIES

Overview

Infrared (IR) is widely used to study the influence of mechanical stress on the molecular structure of polymers. This study used IR

TABLE 1 Relaxation Parameter of Zero Shear Viscosity, η_0, as Obtained from the Relaxation Spectra of the 11 Asphalts Tested

Asphalt Type	Zero Shear Viscosity (Poises)
A	2.95e+05
B	9.16e+05
C	1.78e+07
D	3.14e+06
E	4.23e+06
F	1.17e+06
G	1.19e+06
H	2.59e+06
I	1.89e+06
J	0.49e+06
K	3.76e+06

spectroscopy to evaluate the influence of shearing on the molecular structure of asphalt. Although the detailed chemical knowledge of the interconnectivity of asphalt systems is not known and cannot be determined by this technique, information about the importance of specific bond or group types to mechanical properties can be extracted using rheo-optical techniques. The coupling of IR spectroscopy and controlled shear deformation was introduced by Little et al. (*11*). A detailed introduction to and discussion of analysis through IR spectroscopy is presented by Prapnnachari (*8*).

Experimental Setup

The IR experimental setup included two main units: the IR spectrometer (a Nicolet model 60SXR) and the asphalt shear deformation stage (Minimat marketed by Polymer Laboratory of Massachusetts), which fits in the sample chamber of the Nicolet IR spectrometer and which was used to shear the asphalt in a thin film. A thin-film shearing action, which is similar in concept to the shearing action induced in the thin film of asphalt coating the aggregate particles, is produced by the Minimat setup. While being sheared, the asphalt film was penetrated with an IR beam.

Selection of a proper window material was a key consideration in establishing a transmission IR spectrum. The first criterion to consider in selecting a window material was the frequency range over which the spectrum must be measured. Other important considerations included solubility, reactivity, and refractive index of the window material with respect to the sample. Mechanical and thermal characteristics of the window materials also played a major role in their consideration for this test. Hygroscopic materials such as potassium bromide (KBr) and sodium chloride (NaCl) are used most frequently, primarily because they do not react with organic compounds. Although KBr has a slightly wider spectral range than NaCl, it is too brittle to withstand significant mechanical shocks. Besides, KBr is more hygroscopic and less resistant to thermal fluctuations than NaCl. In this study, NaCl was selected as a window material.

Because of width limitations in the space available for sample holding, a 29- × 14.5- × 4-mm NaCl plate was selected for use. In sample preparation, two such rectangular NaCl plates were coated with a thin layer of asphalt and then sandwiched together. Only one end of each NaCl plate was clamped. The plates remained together under the adhesive influence of the asphalt. To ensure full adhesion to the NaCl plates, a small quantity of asphalt was smeared over one face at a temperature between 60°C and 93°C. The second NaCl plate was pressed firmly by hand over the first, still hot, NaCl plate. This sandwich arrangement was kept at a temperature between 60°C and 93°C in an oven for a few minutes to ensure uniformity. After cooling, the system was placed and clamped in sample holders. Obviously, the portion of NaCl plates under the clamp grip was not coated with asphalt. Subsequently, the entire set was mounted in the sample box of the IR spectrometer.

The maximum available overlap between the two plates through which the IR beam could pass was 13 mm. The number of reproducible IR scans per minute was not greater than six. To optimize the number of IR scans obtained during shearing, a 6-mm/min rate of shear deformation was used. The IR spectral changes below a 4-mm/min deformation rate were hardly perceptible, suggesting that the rate of deformation was slower than the asphalt's characteristic relaxation time, and the spectral changes from 4 to 6 mm/min rate of shearing were identical. The IR spectrometer was programmed so that the first IR scan collected was for the sample with no shear induced. Subsequently, Minimat movement inducing shearing within the asphalt and the IR scan were triggered simultaneously. Figures 1 and 2 show the setup of the IR experiment. Figure 1 is a view of the entire experiment setup (IR spectrometer and Minimat). Figure 2 is a view of the Minimat device, which fits within the chamber of the IR spectrometer and actually shears the asphalt between the NaCl plates while the IR spectra captured during shearing are used to analyze changes in absorbance bands. Prapnnachari (*8*) provides a much more detailed discussion of the experimental setup and the evolution of the approach used.

FIGURE 1 Minimat in Fourier transform infrared spectroscopy chamber.

Infrared Spectral Analysis

IR spectra of asphalts have nine main absorbance bands, which are summarized in Table 2. The absorbance bands are characteristic of a specific molecular structure and its mode of vibration. Absorbance is proportional to the concentration of the chemical group. Asphalt is composed of hydrocarbons, and the band assignments for hydrocarbons are well established in the literature. Primarily using the band assignments for hydrocarbons, Stewart (*13*) and Beitchman (*14*) characterized asphalt bands, as summarized in Table 2. In general, the region of the IR spectrum between 3100 and 2800 cm^{-1} indicates the nature of the hydrocarbon part of a molecule. This region was examined first, since the position of the CH stretching band suggests the structural feature of a hydrocarbon molecule. Absence of absorbance above 3000 cm^{-1} suggests that molecules are aliphatic and alicyclic with no ethylenic or aromatic structure. Figure 3, a typical IR spectrum of an asphalt, shows strong absorbance from 2950 to 2850 cm^{-1}, which suggests the dominance of aliphatic and alicyclic hydrocarbon structures in all the asphalts tested. This does not mean that aromatics are absent in the asphalt molecules. Sometimes the closer

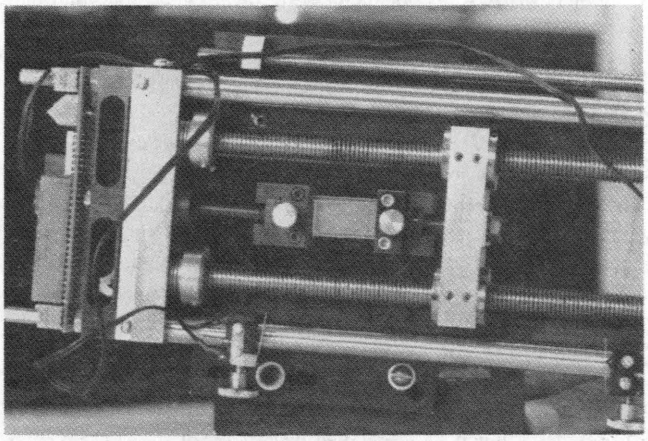

FIGURE 2 Minimat deformation stage.

frequencies develop coupled vibrations, shifting absorbance to unexpected regions of the spectrum. This might occur because of the complex structure of the asphalt molecules. Close examination of the absorbance in the 3000 to 2800 cm^{-1} region indicates the presence of two peaks for aliphatic and alicyclic CH stretching: one near 2850 cm^{-1} (alicyclic) and the other near 2925 cm^{-1} (aliphatic). The steep shoulder near the 3000 cm^{-1} peak indicates weak absorbance due to the aromatics. This peak is obscured by the very strong CH_2 and CH_3 stretching bands during shearing of the aliphatics and alicyclics. Generally, the aromatic structures in a hydrocarbon can be found (*15*) in five regions of the IR spectrum: 3100 to 3000 cm^{-1} for CH stretching, 1650 to 1430 cm^{-1} for C=C stretching, 1275 to 1000 cm^{-1} for in-plane CH bending, 900 to 690 cm^{-1} for out-of-plane CH bending, and 2000 to 1700 cm^{-1} for overtones and combinations. In the IR spectrum of an asphalt, weak absorbance near 1600 cm^{-1} suggests C=C stretching of the aromatics, and small absorbance at 863, 813, and 745 cm^{-1} is due to CH out-of-plane bending. The overtones and in-plane CH bending were not witnessed.

The region near 1460 and 1375 cm^{-1} reveals the presence of methylene and methyl groups. The band near 1460 cm^{-1} indicates the antisymmetric deformation of the HCH angle of a CH_3 molecule. The bending of methylene (CH_2) groups gives rise to a band in the same region. The symmetric CH_3 bending gives a strong, sharp band near 1376 cm^{-1}. A small band near 720 cm^{-1} is indicative of a linear chain containing four or more CH_2 groups. The relative numbers of CH_2 and CH_3 groups are evaluated by the combined study of the 1460, 1376, and 720 cm^{-1} bands. When there are more CH_2 groups than CH_3 groups present, the 1460 cm^{-1} band will be stronger (*15*) than the 1376 cm^{-1} band. A greater relative intensity of the band near 1460 cm^{-1} than 1376 cm^{-1} was found in general in the IR spectra of all the asphalts. This shows the dominance of CH_2 groups over CH_3 groups in the asphalt molecules. The relative length of CH_2 chains among asphalts can be evaluated by the study of absorbance near 720 cm^{-1}, in particular by studying the change in ratio of the CH_2 and CH_3 absorbencies.

Absorbance Peaks

The height and area of an absorbance peak indicate the concentration of a particular molecular component in the sample. For a given asphalt, the ratio of any two absorbance peaks provides the ratio of two representative molecular components present in asphalt. For an identical chemical and mechanical environment, as is noted from Beer's law, the ratio between two peaks is always reproducible irrespective of the number of IR scans and the change in thickness of the sample if the change is uniform. The spectral changes under the influence of mechanical stress on the asphalt sample can thus be quantified by study of the change in the ratio of the absorbance peaks. For a number of spectra, ratios of the peak area were also compared as suggested by Keonig (*16*). In all cases, the peak area ratios verified the results obtained from the evaluation of peak absorbance ratios.

Table 3 gives the absorbance peak ratio of all other bands of the IR spectrum of Asphalt Type A with respect to its 721 cm^{-1} peak for various stages of shearing. As shown in Figure 4, the 1376 to 1457 cm^{-1} bands ratioed with respect to the 721 cm^{-1} band changed appreciably. This is an obvious indication of the key role the chain length plays in asphalt during mechanically

TABLE 2 IR Band Assignments for Asphalt

Wave Numbers (cm^{-1}) S-Strong M-Med. W-Weak	Methyl Groups CH_3 Saturated Aliphatic	Methylene Groups CH_2 Saturated Aliphatic	Aromatic
2950 s	asymmetric stretch	asymmetric stretch	
2860 m	symmetric stretch	symmetric stretch	
1600 w			aromatic ring modes, weak for nonpolar substituents υ (c - c)
1460 m	asymmetric bending	symmetric bending	
1376 m	symmetric bending		
*866 w			1,2,3,4/5 tetra/penta substituted δ (CH)
*813 w			1,4 disubstituted (para) δ (CH)
*745 w			1,2 disubstituted (ortho) or monosubstituted δ (CH)
*720 w		rocking mode $(CH_2)_{n>4}$	monosubstituted δ (CH)

*Aromatic frequencies are more characteristic of the position of the substituents than of their nature.

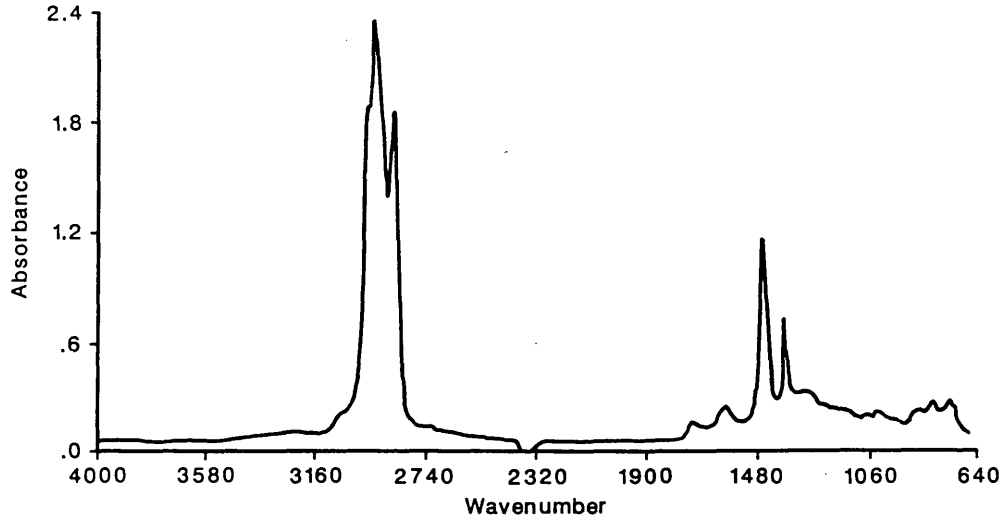

FIGURE 3 IR absorbance spectrum (650 to 4000 cm^{-1}) for unsheared Asphalt Type A.

TABLE 3 Absorbance Peak Ratios, Asphalt Type A

Stretch Stages	Peak ratio with respect to 721 cm^{-1} band				
	745 cm^{-1}	813 cm^{-1}	1376 cm^{-1}	1457 cm	1600 cm^{-1}
1	1.119	1.086	2.924	4.633	1.033
2	1.109	1.082	2.820	4.415	1.037
3	1.120	1.071	2.810	4.447	1.034
4	1.118	1.072	2.703	4.211	1.036
5	1.113	1.069	2.492	3.971	1.046
6	1.122	1.068	2.480	3.772	1.060
7	1.121	1.064	2.273	3.750	1.058
8	1.122	1.057	2.412	3.710	1.056
9	1.124	1.063	2.207	3.734	1.060
10	1.116	1.062	2.412	3.698	1.057

induced shear. Figure 5 is typical of the collective spectra obtained during the stages of shearing for an asphalt (Type K). The change in the shape of the bands and shoulders, mostly near the 745 cm^{-1} band, results from the interaction of substituent CH_2 molecules.

The studies of changes in absorbance peak ratios (Figure 4) and changes in band shapes and shoulders (Figure 5) are complementary. The most affected peak ratios, 1457 and 1376 cm^{-1} bands ratioed with respect to the 721 cm^{-1} band, indicate that CH_2 and CH_3 molecules forming the chains attached to the asphalt molecules are most active in resisting shearing. The change in band shapes and shoulders in the region of the aromatic out-of-plane CH bending absorbance suggests the interaction of the CH_2 chains with the aromatics. This suggests that the network of CH_2 chains forming the substituents to the aromatics also contributes to resisting mechanically induced stress.

WIDE-ANGLE AND SMALL-ANGLE X RAY DIFFRACTION

Principles of Diffraction

X ray diffraction is a tool for the investigation of the fine structure of matter. Early X ray use was limited to the determination of crystal structures. Today, X rays are used not only for crystal structure determination but are also applied to problems in chemical analysis, stress measurement, phase equilibrium, and the measurement of particle size.

Diffraction is produced by the interference of waves scattered by an object. When the X rays strike the object at an angle, 2θ, every electron becomes the source of a scattered wave. If an X ray beam of intensity I_0 interacts with a free electron, the intensity

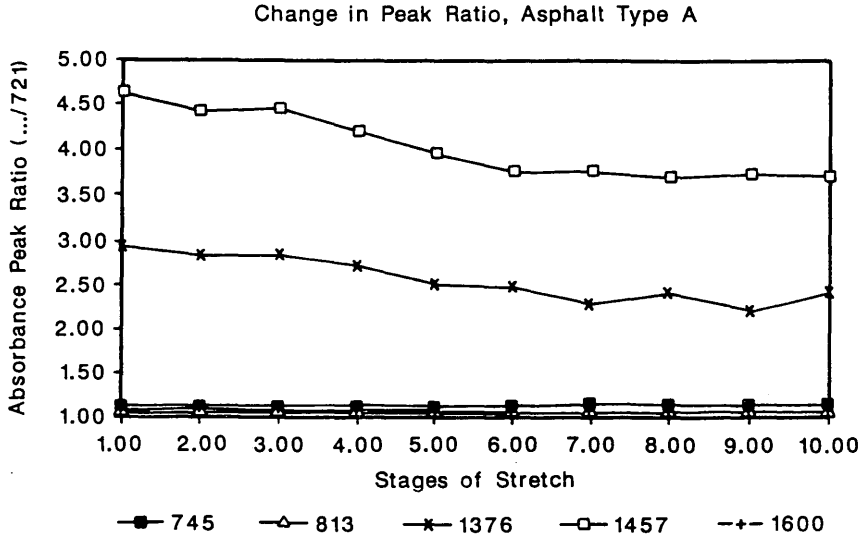

FIGURE 4 Peak ratio versus stage of shearing (mm) for Asphalt Type A.

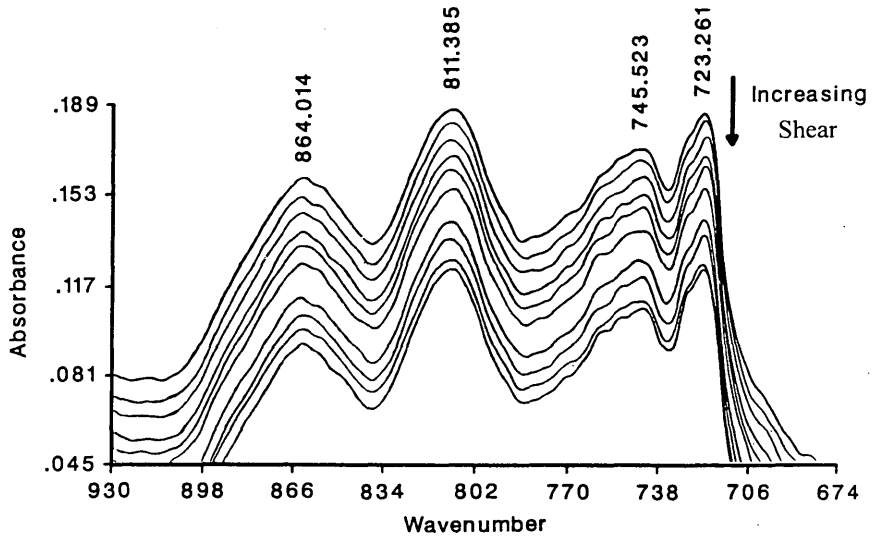

FIGURE 5 Collected IR absorbance spectra (680 to 930 cm^{-1}) for stages of shearing for Asphalt Type K.

I is expressed as

$$I = I_0 \frac{K}{R^2}\left(\frac{1 + \cos^2 2\theta}{2}\right)$$

Here the constant K is defined by e^4/m^2c^4, where e and m are charge and mass of an electron, respectively, and c is the velocity of light. R is the scattering vector.

For a noncrystalline material consisting of a single type of atom, the spatial distribution of atoms can be expressed conveniently by means of a radial distribution function ρ (r), which is described as the number density of atoms to be found at a distance r from the center of any one of the atoms.

If a material contains more than one kind of atom, its amorphous structure can be characterized in principle by a generalized radial distribution function (*17*). From the radial distribution function, the density of atoms or the frequency of separations between atoms can be obtained by analyzing the peaks in the data. This provides a quantitative information source regarding the different atoms such as carbon and hydrogen in asphalt.

X ray scattering techniques are usually categorized into wide-angle X ray scattering (WAXS) and small-angle X ray scattering (SAXS). In WAXS, the structural information is obtained on a scale of 1 nm or smaller. The angle measured is between 3 and 90 degrees. The inhomogeneities of atomic dimensions give rise to WAXS. In SAXS, fluctuations in electron density over large distances, typically 30Å to 1000Å, are determined. The inhomogeneities of colloidal dimensions generate X ray scattering and interference effects at very small angles, typically less than 2 degrees, with the wavelength of CuKα, 1.542Å.

Since WAXS probes atomic dimensions, different bands of X ray beams diffracted from the lattice planes are obtained as intensity. With knowledge of the position of peaks, quantitative information concerning crystalline and amorphous structures can be obtained. Since SAXS identifies large structures, the intensity peaks are spaced according to the distance between large areas of contrasting density. This capability provides a tool by which to determine whether asphalt is a colloid or a network structure.

Use of Fractal Analysis To Determine Asphalt Molecular Topology

Fractal analysis can be used to characterize disordered objects ranging from macromolecules to the earth's surface (*18*). These objects display "dilation symmetry," which means that they look geometrically self-similar under transformation of scale such as changing the magnification of a microscope. Complex structures such as Eden, Vold, Wittne-Sander, and so forth (*19*) can be simply characterized with the single parameter D, the fractal dimension, which is defined as the exponent that relates the mass M of an object to its size R as

$$M \propto R^D \tag{1}$$

where $\propto$ is interpreted as "proportional to" in Equations 1 through 3.

This equation also applies to simple objects such as rods, disks, and spheres, for which the exponent D is equal to 1, 2, and 3, respectively. For fractal objects, however, the exponent need not be an integer.

Polymers are described by Equation 1 and are called "mass fractals." On the contrary, colloids are "surface fractals," which are uniformly dense but have a rough surface. Surface fractals share the self-similarity property; however, if the surface is magnified, its geometric features do not change. Mathematically, surface self-similarity is represented by an analog of Equation 1:

$$S \propto R^{D_s} \tag{2}$$

where S is the surface area and D_s is the surface fractal dimension. For a smooth object, $D_s = 2$, consistent with the notion that a

smooth surface is two dimensional. For fractally rough surfaces, however, D_s varies between 2 and 3, so D_s is a measure of the surface roughness.

Fractals can be characterized by small-angle X ray scattering techniques. The asphalt sample was subjected to X rays, and the angular dependence of the scattered intensity was measured. For fractal objects, the intensity profile has a power law dependence when plotted versus the magnitude of the wave vector K (*20*):

$$I \propto S^{-2D} + D_s \tag{3}$$

The quantity $P = -2D + D_s$ is called the Porod shape. Through Bragg's law, the parameter S can be related to a characteristic length L and the scattering angle θ ($S = 2\pi/L = 4\pi\lambda^{-1}\sin\theta$), where λ is the wavelength. By scanning θ, an object on different length scales can be studied effectively. Though there are exceptions to the general rules (*20*), it is usually possible to distinguish structures by the exponent in Equation 3. Polymeric (mass fractals where $D_s = D$) systems yield scattering curves with slopes between -1 and -3, whereas smooth colloids give slopes of -4. Rough colloids give slopes of between -3 and -4 (*21*). The analysis of the Porod slopes of SAXS curves is shown in Figure 6 for polymeric and colloidal systems.

The method described above was used on four of the SHRP asphalts (AAM, AAD, AAF, and AAK). Figure 7 shows the raw data, empty cell scattering, and absorption data for asphalt AAF-1. Correction for the empty cell scattering and absorption was made as follows:

$$I_{cor} = I_{raw} - (I_{empty\ cell} - I_{abs}) \tag{4}$$

The background correction was made following the method of Ruland (*22*). Figure 8 shows the corrected intensity $I(s)$. The power law scattering, $I(s) \approx S^{-P}$ was observed in the range of -7 to -4 of ln s. The exponent P was determined to be -0.8 by the least squares method (Figure 9). This is consistent for all asphalts studied, suggesting a noncolloidal, linear system.

EVALUATION OF RELAXATION MECHANISM

The changes in the molecular structure of asphalts were observed in the collective IR absorbance spectra during shearing state; the perturbations and shoulders at random frequencies indicative of the region of substituents to the aromatics demonstrate the conformational changes to the appendages of the aromatics (Figure 5). Figure 4 shows that most of the changes occur in the peak ratio of the CH_2 and CH_3 bands (721, 1376, and 1457 cm^{-1}). The shearing of the asphalt sample in the IR beam indicates that the methylene structures, irrespective of their position in the molecule (Figure 4), are most active in resisting mechanically induced stress. The band at 721 cm^{-1} is for skeletal rocking of CH_2 molecules; the band at 1376 cm^{-1} represents the symmetrical bending mode vibration of CH_3 molecules; the band at 1457 cm^{-1} represents the combined symmetrical and asymmetrical bending modes of vibration of CH_2 and CH_3 molecules, respectively.

The length of a methylene chain structure is represented by the ratio of CH_2 and CH_3 groups. During deformation, the $[CH_3]/[CH_2]$ absorbance ratio may decrease because of an increase in $[CH_2]$ at fixed $[CH_3]$ concentration or because of a decrease in the $[CH_3]$ concentration. We cannot distinguish one mechanism from the other and therefore cannot state which occurs. But it is clear that the higher the ratio in the undeformed state, the longer the representative chain length. The changes observed in the ratio of the peaks of the absorbance bands during deformation offered qualitative information only. No fixed pattern or reproducibility was observed for each stage of shear deformation on replicates of the asphalt samples. Random changes in the peak ratio were shown that indicate high randomness in the orientation and length of asphalt chains. The observation shown in Figure 4 suggests that the changes under mechanically induced shearing are due to interactions among and within methyl and methylene molecules. The extent of these changes could not be quantified because the asphalts studied possess random orientation of the short methylene chains. The representative chain length of the asphalt molecule represented by the ratio of CH_2 (721 cm^{-1}) to CH_3 (1376 cm^{-1})

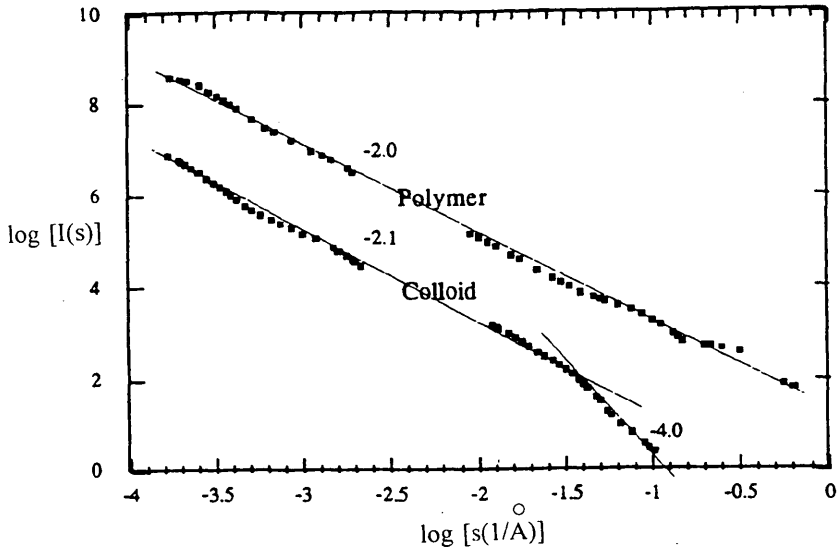

FIGURE 6 Contrasting SAXS profiles for polymeric and colloidal systems.

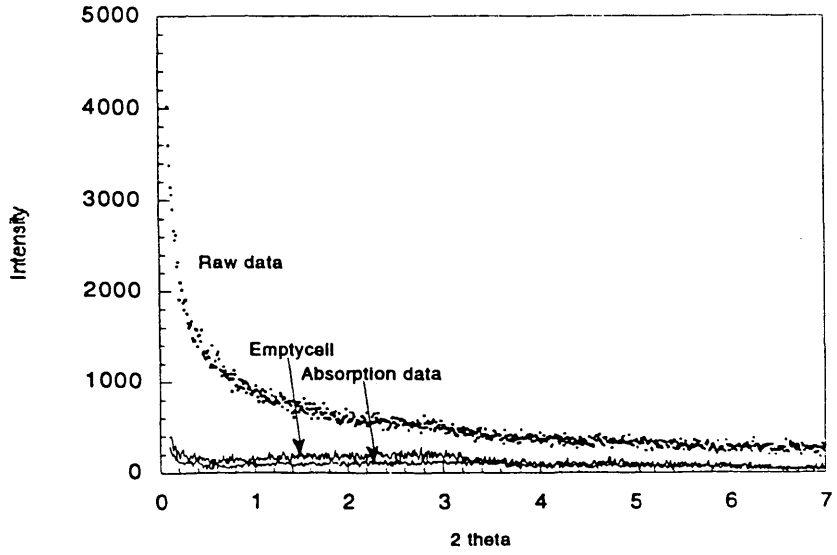

FIGURE 7 SAXS curves of AAM asphalt raw data, empty cell scattering, and absorption data.

absorbance of the undeformed sample is given in Table 4. Stewart (*13*) suggested this absorbance as indicative of the presence of bulk assemblies of aliphatic hydrocarbon chains in an asphalt molecule.

The viscoelastic characteristics of the asphalts were evaluated by the relaxation spectrum obtained from the master curves of the storage and loss moduli. The master curves were constructed from analysis of the dynamic mechanical test data explained previously. The experiment was carried out over the temperature range −25°C to 65°C, and the master curves were constructed at a reference temperature of 25°C. The absence of the rubbery plateau in the master curves of the asphalts suggests a single relaxation transition for asphalts. This indicates that the asphalts may demonstrate a polymeric solution type behavior.

Figure 10 shows the dependence of the relaxation time of asphalts on their representative chain length. The slope of the log zero shear viscosity and log CH_2/CH_3 plot is 4.2 with considerable scatter among the data. The relaxation model (*23–25*) for polymeric solutions suggests a slope of 3.45. Since these values are within statistical significance (the 95 percent confidence interval for the slope calculated between zero shear viscosity and chain length is ±0.9), we can conclude that an entangled polymerlike solution exists. Since asphalts are low-molecular-weight hydrocarbons, an explanation for this behavior is needed. A dependence

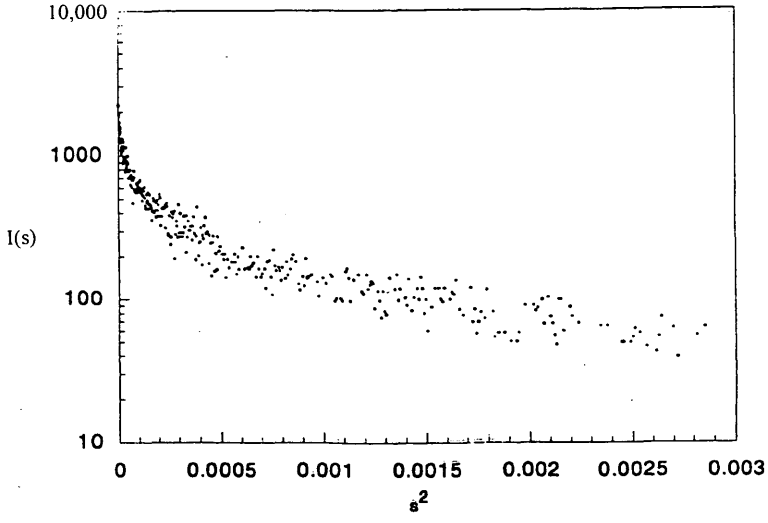

FIGURE 8 Log *I* versus s^2 plot of the SAXS curve of AAM asphalt.

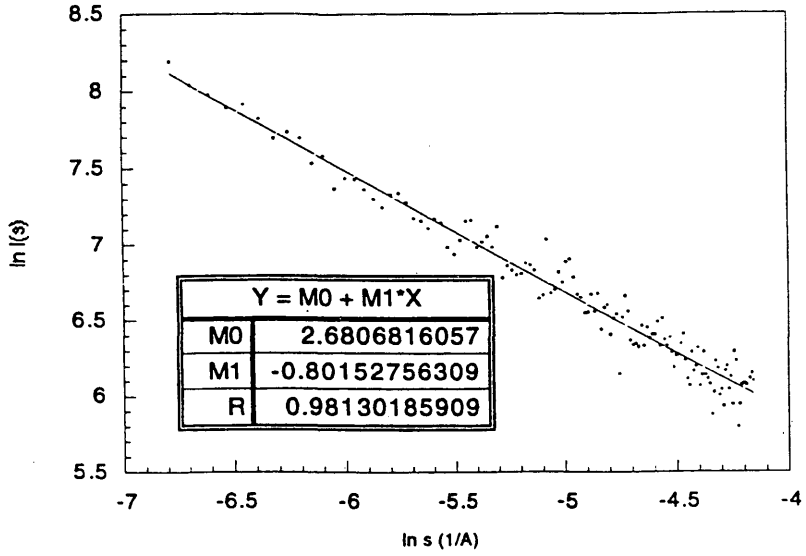

FIGURE 9 Log-log plot of the SAXS curve for AAM asphalt.

of the relaxation behavior of the asphalts on chain length was observed, suggesting a possible "virtual" network that extends linear interactions by producing virtual cross-links or entanglements. Surprisingly few of these interactions are needed to produce the observed viscoelastic behavior. The deviation from polymer solution behavior indicates that the asphalts are also strongly influenced by their dispersed structure.

The 11 asphalts previously discussed were analyzed to determine whether Corbett compositional analysis is related to the zero shear viscosity value of the asphalt. However, no component of the Corbett fraction can by itself explain the physical behavior of asphalt (Table 4). A plot of unrelaxed modulus (G_R) of the asphalts studied (unrelaxed modulus is obtained from discrete relaxation spectra at an infinitely small time common to all the asphalts) in Figure 11 demonstrates a rough correlation (except the Asphalt Type J) between representative chain lengths in the asphalt and relaxation time. Asphalt Type J, although having an abnormally high initial modulus, does not maintain the long-term resistance to flow; its initial high modulus might be due to highly polar and interactive asphaltene fractions. Table 3 indicates that Type A asphalt has the highest asphaltene percentage. But since Asphalt A has the smallest representative methylene chain length, it lacks the long-term potential of resistance to flow.

CONCLUSIONS

The objective of this study was to probe the relationship between an asphalt's structure and the viscoelastic properties observed for

TABLE 4 Values of the Ratio of Peak Absorbance of CH_2 (721 cm^{-1}) to CH_3 (1376 cm^{-1}) and Relaxation Strength of the Asphalts

Asphalt Type	Ratio of CH_2 (721 cm^{-1}) to CH_3 (1376 cm^{-1}) Absorbance	Zero Shear Viscosity (Poises)
A	0.342	2.95e+05
B	0.284	9.16e+05
C	0.624	1.78e+07
D	0.409	3.14e+06
E	0.412	4.23e+06
F	0.386	1.17e+06
G	0.406	1.19e+06
H	0.397	2.59e+06
I	0.384	1.89e+06
J	0.288	0.49e+06
K	0.376	3.76e+06

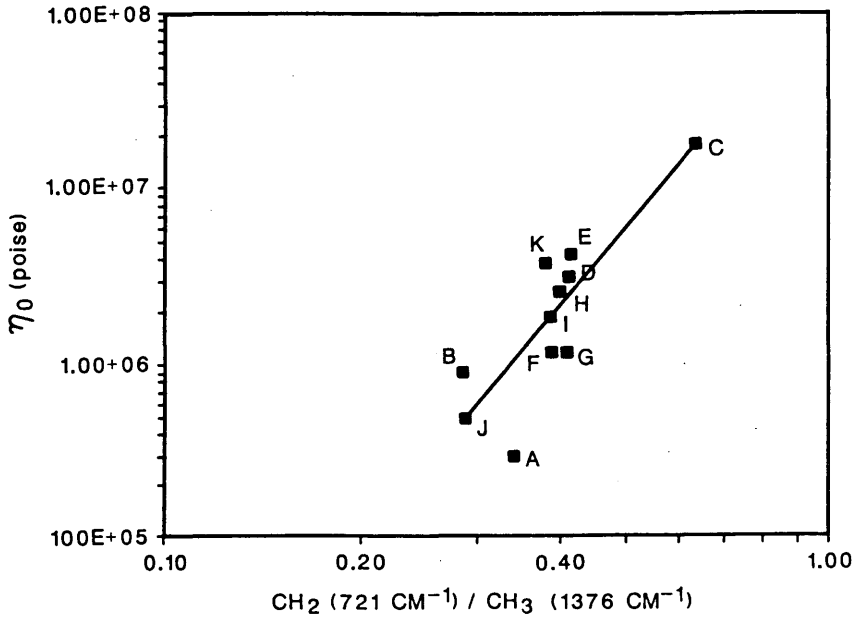

FIGURE 10 Chain length dependence of relaxation strength of the asphalts studied. η_0 is the zero shear viscosity.

the asphalt. The bulk assemblies of the methylene chains in asphalts were observed to be most active in resisting mechanically induced stress. This result is concluded from the rheo-optical studies in which specific IR bands were observed to change during shear deformation of the asphalt. The ratio of methylene to methyl absorbance in the IR spectrum offered a method of evaluating the representative length of the methylene chains in an asphalt. The methyl and methylene absorbance bands used for the study were 1376 and 721 cm^{-1}, respectively. The methylene band, 721 cm^{-1}, represents aliphatic $(CH_2)_{n>4}$ hydrocarbons in asphalts. Using this information, a correlation between the asphalt's chain "length" and the viscoelastic properties of these materials was determined. In particular, the relaxation spectrum of asphalt was used to evaluate the zero shear viscosity, which is a measure of long-term resistance to flow. The study demonstrated the dependence of the asphalt's long-term resistance to flow on the representative length of the methylene chains. It is important to note the relationship previously discovered by Benson and Little (*26*) between meth-

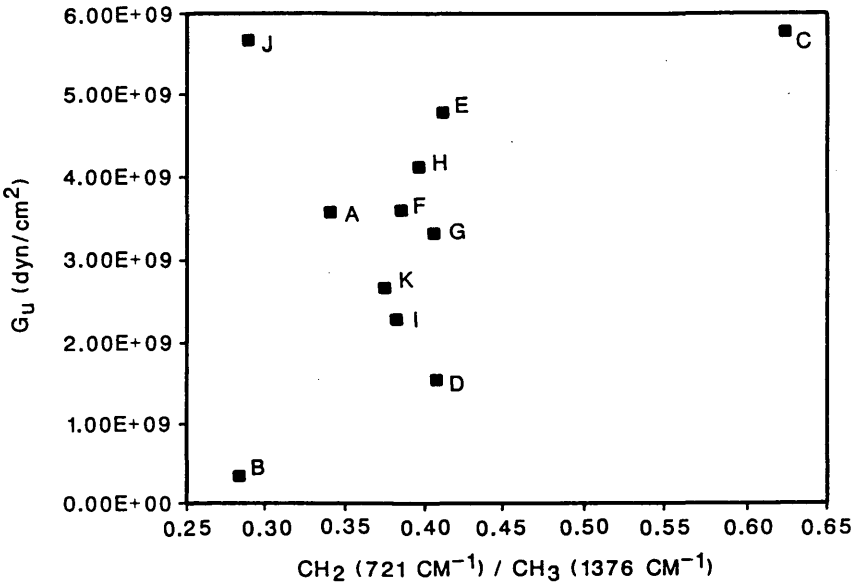

FIGURE 11 Unrelaxed relaxation strength versus chain length of the asphalts studied.

ylene chain length (methylene to methyl ratio) and microdamage healing. In the Benson and Little work, longer methylene chains resulted in superior microdamage healing.

The plot of the log of the representative length of the methylene chains versus log of the zero shear viscosity showed considerable scatter with a correlating slope of 4.2. As reported in the literature, for true polymeric solutions a slope of 3.45 should be observed. From the data, there is no ($\alpha = 0.05$) statistical difference between 4.2 and 3.45, suggesting a possible solution type behavior with chain entanglements.

These data suggest that a model supporting a colloid type structure is unlikely. The X ray data do not suggest the existence of colloid structures (in the range detectable from X ray analysis) but instead suggest the dominance of linear type structures. This is in agreement with the rheo-optical data, suggesting that "linear" structures control the viscoelastic deformation of these materials. These linear structures are interconnected through a virtual network providing the structure needed to justify the observed mechanical properties. This proposed organization is not unlike the DPF model. The polar interactions form the virtual network with a number of linear structures (appendages to the aromatic structures) thereby controlling the viscoelastic nature of the asphalt. More work is needed to further investigate this phenomenon.

REFERENCES

1. Corbett, L. W. Composition of Asphalt Based on Generic Fractionation Using Solvent Deasphaltening, Elution-Adsorption Chromatography, and Densimetric Characterization. *Analytical Chemistry*, Vol. 41, 1969, pp. 576–579.
2. Dealy, J. M. Rheological Properties of Oil Sand Bitumens. *Canadian Journal of Chemical Engineering*, Vol. 57, 1979, pp. 677–683.
3. Boduszynski, M. M., J. F. McKay, and D. R. Latham. Asphaltenes, Where Are You? *Proc., Association of Asphalt Paving Technologists*, Vol. 49, 1980, pp. 123–143.
4. Petersen, J. C. Chemical Composition of Asphalt as Related to Asphalt Durability—State of the Art. Presented at 63rd Annual Meeting of the Transportation Research Board, Washington, D.C., 1984.
5. Halstead, W. J. Relation of Asphalt Chemistry to Physical Properties and Specifications. *Proc., Association of Asphalt Paving Technologists*, Vol. 54, 1985, pp. 91–117.
6. *Binder Characterization and Evaluation.* Quarterly Report, Technical Section, SHRP A-002A. Western Research Institute, University of Wyoming Research Corporation, Laramie, June 1991.
7. Monismith, C. L. *Asphalt Paving Mixtures Properties, Design, and Performance.* Course notes, Short Course in Asphalt Paving Technology. The Institute of Transportation and Traffic Engineering, University of California, 1961.
8. Prapnnachari, S. *Investigation of Microstructural Mechanism of Relaxation in Asphalt.* Ph.D. dissertation. Texas A&M University, College Station, 1992.
9. Walters, K. *Rheometry.* John Wiley and Sons, New York, 1975.
10. Barnes, H. A., J. F. Hutton, and K. Walters. *An Introduction to Rheology.* Elsevier Science Publishing Company, New York, 1989.
11. Little, D. N., S. Prapnnachari, A. Letton, and Y. R. Kim. *Investigation of the Microstructural Mechanisms of Relaxation and Fracture Healing in Asphalt.* Final Report, Grant AFOSR-89-0520. Texas Transportation Institute, Texas A&M University, College Station, 1993.
12. Baumgaertel, M., and W. H. Winter. Determination of Discrete Relaxation and Retardation Time Spectra from Dynamic Mechanical Data. *Reologica Acta*, Vol. 18, No. 6, 1989, pp. 511–579.
13. Stewart, J. E. Infrared Spectra of Chromatographically Fractionated Asphalts. *Journal of Research of the National Bureau of Standards*, Vol. 58, No. 5, 1957, pp. 265–269.
14. Beitchman, B. D. Infrared Spectra of Asphalts. *Journal of Research of the National Bureau of Standards*, Vol. 63A, No. 2, 1959, pp. 189–193.
15. Lambert, J. B., H. F. Shurvell, D. A. Lightner, and R. G. Cooks. *Introduction to Organic Spectroscopy.* Macmillan Publishing Company, New York, 1987.
16. Keonig, J. L. *Spectroscopy of Polymers.* American Chemical Society, Washington, D.C., 1991.
17. Alexander, L. E. *X-Ray Diffraction Methods in Polymer Science.* R. E. Publishing Company, Malabar, Fla., 1985.
18. Mandelbrot, B. B. *The Fractal Geometry of Nature.* Freeman, San Francisco, Calif., 1982.
19. Schaefer, D. W. *Science*, 243, 1023, 1989.
20. Martin, J. E., and A. J. Hurd. *J. Appl. Cryst.*, 20, 61, 1987.
21. Bale, H. D., and P. W. Schmidt. *Phys. Rev. Lett.*, 53, 596, 1984.
22. Ruland, W. *Pure Appl. Chem.*, 49, 505, 1977.
23. De Gennes, P. G. *Introduction to Polymer Dynamics.* Cambridge University Press, New York, 1990.
24. Doi, M., and S. F. Edwards. *The Theory of Polymer Dynamics.* Clarendon Press, Oxford, New York, 1986.
25. Aklonis, J. J., and W. J. MacKnight. *Introduction to Polymer Viscoelasticity* (2nd edition). John Wiley and Sons, New York, 1983.
26. Benson, F. C., and D. N. Little. *Correlation Among Asphalt Concrete Mechanical Healing, Asphalt Cement Dispersion, FTIR Chemical Functional Groups and ^1H NMR Chemical Structure.* Final Report, Grant ECE-8511851. National Science Foundation, 1988.

Publication of this paper sponsored by Committee on Characteristics of Bituminous Materials.